Theory of superconductors with κ close to $1/\sqrt{2}$

I. Luk'yanchuk
L. D. Landau Institute for Theoretical Physics, Moscow, Russia
and Institut für Theoretische Physik, RWTH-Aachen, Templergraben 55, D-52056 Aachen, Germany
(Received 26 October 2000; published 3 April 2001)

As was first shown by Bogomolnyi, the critical Ginzburg-Landau (GL) parameter $\kappa = 1/\sqrt{2}$ at which a superconductor changes its behavior from type I to type II, is the special highly degenerate point where Abrikosov vortices do not interact and therefore all vortex states have the same energy. Developing a secular perturbation theory, we studied how this degeneracy is lifted when κ is slightly different from $1/\sqrt{2}$ or when the GL theory is extended to the higher terms in $T - T_c$. We constructed a simple secular functional that depends only on few experimentally measurable phenomenological parameters and therefore is quite efficient to study the vortex state of superconductor in this transitional region of κ. On this base, we calculated such vortex state properties as critical fields, energy of the normal-superconductor interface, energy of the vortex lattice, vortex interaction energy, etc., and compared them with previous results that were based on bulky solutions of GL equations.

DOI: 10.1103/PhysRevB.63.174504 PACS number(s): 74.60.Ec, 74.20.De, 74.55.+h, 74.60.−w

I. INTRODUCTION

Although the Ginzburg-Landau (GL) theory covers all the varieties of superconductors, both of the type I with GL parameter $\kappa < 1/\sqrt{2}$ and of the type II with $\kappa > 1/\sqrt{2}$, most of the theoretical studies of the vortex state deal with the case of $\kappa \gg 1/\sqrt{2}$ since at $\kappa \gg 1/\sqrt{2}$ the GL equations are simplified substantially and also the grand majority of type II superconducting materials including high-T_c superconductors correspond to this limit.

Studies of superconductors in the transitional region of small $\kappa \sim 1/\sqrt{2}$ done mostly in the 1970s were based on the solution of the full system of GL equations and require bulky calculations. Meanwhile, Bogomolnyi proposed in 1976 an elegant way to operate with similar problem of the string theory[1] and showed that at the special point $\kappa = 1/\sqrt{2}$ the order of the equations can be reduced and all the vortex states with arbitrary located vortices have the same energy when the applied field is equal to the critical field H_c.

Historically the Bogomolnyi approach was done for the high-energy physics and the superconducting community was not aware of it even when Jacobs and Rebbi[2] reformulated the Bogomolnyi equations in terms of superconductivity and demonstrated that they can be written in a form of nonlinear electrostatic equation of the Boltzman plasma that we call Bogomolnyi, Jacobs, and Rebbi (BJR) equation. Only very recently the Bogomolnyi method was used to study vortices in mesoscopic disks[3] and to calculate the structure of multiquanta vortices[4] in superconductors with $\kappa = 1/\sqrt{2}$.

In the present paper we derive a regular way to treat the vortex state of superconductors with κ close to $1/\sqrt{2}$ based on the BJR approach. Our basic idea is to consider the highly degenerate Bogomolnyi state at $\kappa = 1/\sqrt{2}$ and $H = H_c$ as zero approximation and then to account for a deviation from this point via the secular perturbation method that lifts the degeneracy and selects the most stable vortex configuration. In Sec. III we give a brief overview of the Bogomolnyi method and then, in Sec. IV, present the solutions the of BJR equation for the different vortex lattices. In Sec. V we develop the secular perturbation approach. The following perturbations can lift the degeneracy.

(i) Deviation of κ from $1/\sqrt{2}$ that is accounted by a small parameter.

$$\gamma = \kappa^2 - \frac{1}{2} \approx \sqrt{2}\kappa - 1. \tag{1}$$

(ii) Deviation of the applied field from H_c.

(iii) Next in

$$t = T/T_c - 1, \tag{2}$$

corrections to the GL functional.

(iv) Thermal fluctuation effects.

(v) Finite size and demagnetization effects.

We consider only the first three contributions and show that they can be incorporated in a very simple secular functional that acts on the Bogomolnyi degenerate solutions and looks like a six-order polynomial for the amplitude of the order parameter. This functional depends only on few phenomenological parameters that can be found from experiments and that completely determine the behavior of superconductors with $\kappa \sim 1/\sqrt{2}$ in a magnetic field.

Certain properties of superconductors with $\kappa \sim 1/\sqrt{2}$ were calculated either from the GL theory extended to low temperatures or from the microscopic Gorkov equations. These calculations, overviewed in Sec. II, were however dealing either with cumbersome analytical expansions or with numerical computations that both are difficult to catch on. It is therefore of interest to recalculate these properties in a systematic perturbation way and compare them with the older results.

In Sec. VI we calculate the following parameters of a superconductor with $\kappa \sim 1/\sqrt{2}$: (a) critical fields H_{c1}, H_{c2} and H_c, (b) energy of the normal-superconducting (N-S) interface, (c) energy of the regular vortex lattice as a function of the applied field, (d) Energy of the N-quanta vortex, (e) vortex interaction that can have an unconventional attractive character.

Based on these calculations we discuss the possible scenarios of the normal-superconducting (NS) transition in a magnetic field for a superconductor with $\kappa\sim 1/\sqrt{2}$ (Sec. VII) that occurs either directly (like in a type-I superconductor) or via the formation of the intermediate vortex (V) state (like in a type-II superconductor). The actual scenario depends on the relative strength and sign of coefficients in the perturbation functional that can be extracted from experiment. We calculate the location of the triple point L on the H-T plane where the direct N-S transition splits into N-V and V-S transitions and a superconductor changes its behavior from type I to type II. The important feature is that both the N-V and V-S transitions close to point L can be either continuous or discontinuous unlike the traditional type-II superconductor with $\kappa \gg 1/\sqrt{2}$ where these transitions are continuous. We calculated the location of tricritical points T_2 and T_1 where the N-V and V-S transitions change their character from continuous to discontinuous.

II. PREVIOUS STUDY

A. Theory

Already in his pioneering work[5] Abrikosov noted that the solution of the GL equations at $\kappa\sim 1/\sqrt{2}$ is a separate and quite complicated problem. Since then, various related theoretical investigations that are partially reviewed in Refs. 6–8 were done. The first series of investigations dealt with an expansion of the BCS free energy close to H_{c2} over a small parameter $H-H_{c2}$. The magnetic and thermodynamic properties of superconductor close to H_{c2} were calculated for dirty[9,10] and intrinsic[11] superconductors. The most complete calculations of this type are given in Ref. 12. The possibility to have a discontinuous N-V transition in a superconductor with $\kappa\sim 1/\sqrt{2}$ was first indicated in Ref. 9.

On the basis of the BCS theory Tewordt and Neumann calculated the low-temperature corrections to GL functional[13–15] and found the upper[16] and lower[15] critical fields with an accuracy t^2 at arbitrary κ.

Based on this extended GL functional, Jacobs[17] considered a superconductor with $\kappa\sim 1/\sqrt{2}$ and calculated the N-S interface energy, the energy of single- and double-quantized vortex. He obtained that at certain conditions the vortices in a type-II superconductor attract each other and predicted the discontinuity of the V-S and N-V transitions. The analogous result was also obtained by Hubert.[18]

Großmann and Wissel[19] calculated the free energy of a superconductor with $\kappa\sim 1/\sqrt{2}$ close to H_{c2} using the extended (although not complete) functional of Tewordt and Neumann. They found a discontinuity of V-S transition in a limit of the dense vortex lattice. All the above conclusions were reproduced by Brandt[20] who developed a variational numerical method to solve the Gorkov's equation for vortex lattices for all possible values of H, T, and κ.

Recently Ovchinnikov[21] carefully derived the coefficients of the extended GL functional from a microscopic theory for different types of electron scattering. He considered an expansion of the free energy near H_{c2} up to the order of $(H-H_{c2})^3$ and specified the case when at $\kappa\sim 1/\sqrt{2}$ the N-V transition has a discontinuous character.

In the present paper we reproduce the above results in a more simple way, based on the Bogomolnyi treatment of superconductors with $\kappa=1/\sqrt{2}$.

B. Experiment

The superconducting metals Ta, Nb, In, and Pb with κ close to $1/\sqrt{2}$ were intensively studied in the 1960s and 1970s. The variation of κ was achieved either by dissolving of foreign atoms of N, Tl, and Bi or by preparation of samples with different defect concentration. We refer to magnetic,[22] calorimetric,[23] and neutron diffraction[24,25] experiments in pure Nb ($\kappa\sim 0.85$–0.96); to magnetic measurements in TaN ($\kappa\sim 0.35$–1.53),[26] in Nb ($\kappa\sim 0.78$–1.03),[26] and in InBi ($\kappa\sim 0.76$–1.46);[27] and to direct observation of vortices in PbTl ($\kappa\sim 0.43$–1.04) (Ref. 28) and in PbIn ($\kappa\sim 0.76$–1.46) (Refs. 29 and 30 by decoration. References to other related experiments can be found in Refs. 6 and 7.

The fact that the V-S transition can be of the first order at $\kappa\sim 1/\sqrt{2}$ was discovered already in the early magnetic and thermodynamic experiments.[22,23,27] The detailed magnetic study of a superconductor that changes its behavior from type I to type II was done for tantalum samples with some amount of dissolved nitrogen[26]. A discontinuity of the vortex lattice parameter at the V-S transition was observed in neutron-scattering experiments.[24,25]

The convincing confirmation of discontinuity of the V-S transition in superconductors with $\kappa\sim 1/\sqrt{2}$ was done by a direct observation of the vortex domains inside the Meissner phase.[28–30] Such coexistence of different phases is known to be a signature of the first-order transition between them. This intermediate-mixed domain structure was interpreted in Ref. 28 in terms of a long-range vortex attraction.

The discontinuity of the V-S transition provided by an attractive interaction between vortices is therefore a well-established fact. Meanwhile, the ground state of the vortex lattice and the configuration of domains of the mixed-intermediate phase are still unclear. Although the decoration experiments[6,7,28–30] allow to observe the very peculiar magnetic textures including vortex segregation and clustering into lamellar and droplike domains, no systematic study of this question that take into account the demagnetization and finite-size effects was done. We believe that our calculations of the vortex energy in the bulk superconductor with $\kappa\sim 1/\sqrt{2}$ can be extended to simulation of magnetic textures in the realistic finite-size samples.

III. GL FUNCTIONAL AT $\kappa^2=1/2$ AND BJR EQUATION

In this section we describe the Bogomolnyi procedure[1] that allows to simplify the GL functional and to reduce the order of the GL equations at $\kappa=1/\sqrt{2}$. Jacobs and Rebbi[2] formulated the Bogomolnyi equations in a simple form of the nonlinear Poisson equation that we shall call the BJR equation. We discuss the properties of the vortex solutions of the

BJR equation and their interpretation in terms of electrons in Boltzman plasma given in Ref. 4.

We start from the conventional GL functional

$$\mathcal{F}=\alpha|\Psi|^2+\frac{g}{2}|\Psi|^4+K|\mathbf{D}\Psi|^2+\frac{B^2}{8\pi}-\frac{BH_0}{4\pi}, \quad (3)$$

where

$$\alpha=\alpha_1 t, \quad \mathbf{D}=\nabla-i\frac{2e}{c\hbar}\mathbf{A}, \quad \mathbf{B}=\mathrm{rot}\ \mathbf{A}$$

Refer first to the characteristic parameters of a superconductor. In the uniform state the superconducting order parameter takes the equilibrium value

$$\Psi_0=\left(-\frac{\alpha}{g}\right)^{1/2}. \quad (4)$$

The ratio of the penetration depth and coherence length

$$\delta=\left(-\frac{c^2\hbar^2}{32\pi Ke^2}\frac{g}{\alpha}\right)^{1/2}, \quad \xi=\left(-\frac{K}{\alpha}\right)^{1/2} \quad (5)$$

gives the GL parameter

$$\kappa=\frac{\delta}{\xi}=\frac{1}{(32\pi)^{1/2}}\frac{c\hbar g^{1/2}}{|e|K}. \quad (6)$$

The thermodynamic critical field and the upper critical field are written as

$$H_c=-\left(\frac{4\pi}{g}\right)^{1/2}\alpha, \quad H_{c2}=-\frac{c\hbar}{2|e|D}\alpha=\sqrt{2}\kappa H_c. \quad (7)$$

Note that the commonly used expression for the low critical field

$$H_{c1}=\frac{\Phi_0}{4\pi\delta^2}\ln\kappa=H_c\frac{\ln\kappa}{\sqrt{2}\kappa} \quad (8)$$

is valid for $\kappa\gg 1/\sqrt{2}$ and is not applicable in our case. The corresponding expression for H_{c1} at $\kappa\sim 1/\sqrt{2}$ will be obtained in Sec. VI. We introduce now the dimensionless variables that are slightly different from the ones commonly used in the GL theory.

$$\psi=\frac{\Psi}{\Psi_0}, \quad r=\frac{R}{\delta\sqrt{2}},$$

$$b=\sqrt{2}\kappa\frac{B}{H_c}, \quad h_0=\sqrt{2}\kappa\frac{H_0}{H_c}, \quad \mathbf{a}=\frac{\kappa\mathbf{A}}{\delta H_c},$$

$$f=\frac{\mathcal{F}}{H_c^2/8\pi}\kappa^2+\kappa^2. \quad (9)$$

The GL functional (3) in this variables takes the form

$$f=\kappa^2(|\psi|^2-1)^2+|(\nabla-i\mathbf{a})\psi|^2+\left(\frac{b^2}{2}-bh_0\right). \quad (10)$$

It is convenient to use the complex variables

$$\zeta,\bar{\zeta}=x\pm iy, \quad (11)$$

$$\partial,\bar{\partial}=\frac{1}{2}(\nabla_x\mp i\nabla_y),$$

$$a,\bar{a}=\frac{1}{2}(a_x\mp ia_y)$$

in which the GL functional is written as

$$f=2|(\partial-ia)\psi|^2+2|(\bar{\partial}-i\bar{a})\psi|^2 \quad (12)$$

$$+\kappa^2(|\psi|^2-1)^2+\left(\frac{b^2}{2}-bh_0\right) \quad (13)$$

To catch the special properties of the GL functional at $\kappa=1/\sqrt{2}$, one can integrate the first term in Eq. (12) by parts. Using

$$\int f\bar{\partial}g\,dS=-\int g\bar{\partial}f\,dS+\frac{i}{2}\oint fg\,d\bar{\zeta} \quad (14)$$

and

$$b=-2i(\partial\bar{a}-\bar{\partial}a) \quad (15)$$

one gets the substitution

$$2|(\partial-ia)\psi|^2\to 2|(\bar{\partial}-i\bar{a})\psi|^2+|\psi|^2 b. \quad (16)$$

We neglect the contribution of the surface currents that are important for finite-size effects considered in Ref. 3. Finally, one comes to the alternative expression for f,

$$f=4|(\bar{\partial}-i\bar{a})\psi|^2+\frac{1}{2}(b+|\psi|^2-1)^2$$

$$+\gamma(|\psi|^2-1)^2+(1-h_0)b, \quad (17)$$

where $\gamma=\kappa^2-1/2$. When $\gamma=0$ and $h_0=1$ (i.e., $H=H_c$) the functional (17) reduces to the sum of two square terms. The absolute minimum is achieved when these terms are equal to zero, i.e., when the following equations are satisfied:

$$(\bar{\partial}-i\bar{a})\psi=0 \quad (18)$$

and

$$1-\psi\bar{\psi}=-2i(\partial\bar{a}-\bar{\partial}a)=b. \quad (19)$$

Substitution of $\bar{a}$ from Eq. (18),

$$\bar{a}=-i\bar{\partial}\ln\psi \quad (20)$$

to Eq. (19) gives the BJR equation

$$\frac{1}{2}\nabla^2\ln|\psi|^2=|\psi|^2-1+2\pi\sum N_i\delta(\mathbf{r}-\mathbf{r}_i). \quad (21)$$

First introduced in Ref. 4, the δ-function terms correspond to the N_i-quanta vortices located at $\mathbf{r}=\mathbf{r}_i$ where ψ gets the phase wind $2\pi N_i$ and $\ln|\psi|$ has a $\ln r^N$ singularity. As follows from Eq. (19), the distribution of magnetic field inside a sample is uniquely related with the amplitude of the order parameter

$$b(\mathbf{r})=1-|\psi(\mathbf{r})|^2. \tag{22}$$

The BJR equation can be alternatively written as

$$\nabla^2\varphi=e^{2\varphi}-1+2\pi\sum N_i\delta(\mathbf{r}-\mathbf{r}_i), \tag{23}$$

where $\varphi=\ln|\psi|$. This form has a simple interpretation.[4] It describes the screening of electrons in a classical Boltzman plasma that consists of the positive ionic background with potential $1/4\pi$.

The BJR equation (21) defines the amplitude of the superconducting order parameter $|\psi(\mathbf{r})|$ and the magnetic field $b(\mathbf{r})$at $\gamma=0$ and at $h_0=1$ as a function of position of the vortices $\mathbf{r}_1,\ldots,\mathbf{r}_n$. All these vortex solutions correspond to the absolute minimum of the functional (17) and, therefore, $\gamma=0$ and $h_0=1$ is a special highly degenerate point where all the vortex states have the same energy.

This infinite degeneracy over $\mathbf{r}_1,\ldots,\mathbf{r}_n$ is lifted if one goes either beyond $\gamma=0$ and $h_0=1$ or beyond the GL approximation. When $\gamma=0$ and $h_0>1$ the absolute minimum of Eq. (17) is the normal state with $b=h_0$ and $|\psi|=0$. When $\gamma=0$ and $h_0<1$ the absolute minimum of Eq. (17) is the uniform superconducting state with $b=0$ and $|\psi|=1$. To find the vortex states when $\gamma\neq 0$, one should account for the term $\gamma(|\psi|^2-1)^2$ as the secular perturbation that lifts the degeneracy. This will be done in Sec. V together with an account of the low-temperature corrections to the GL functional.

IV. VORTEX STATE AT $\kappa^2=1/2$

A. General

In this section we discuss the particular class of solutions of BJR equation (21) when $N-$ quanta vortices are packed into the regular lattice with basis vectors $\mathbf{a}_1$ and $\mathbf{a}_2$. We will need these solutions in Sec. VI as zero approximation of the perturbation theory to find the most stable vortex configuration beyond the Bogomolnyi point. The unit cell area $S=a_1a_2\sin\alpha$ ($\alpha=\mathbf{a}_1\widehat{\ }\mathbf{a}_2$) carries the flux $2\pi N$ and therefore is related with the average induction as

$$S=2\pi N/\overline{b}. \tag{24}$$

The value of $\overline{b}$ and S varies from $\overline{b}=0$, $S=\infty$ (almost nonoverlapping vortices) to $\overline{b}=1$, $S=2\pi N$ (dense vortex lattice). We consider both limits analytically. We use a numerical procedure to treat the case of an arbitrary lattice.

B. One vortex

The axially-symmetric distribution of the order parameter $g_N(r)=|\psi(r)|$ inside the N-quanta vortex is calculated from the radial version of BJR equation (21),

$$g_N''=\frac{g_N'^2}{g_N}-\frac{g_N'}{r}+g_N^3-g_N \tag{25}$$

with the boundary conditions $g_N(0)=0$, $g_N(\infty)=1$ and asymptotes

$$g_N\simeq B_Nr^N,\quad r\to 0, \tag{26}$$

$$g_N\simeq 1-A_N\frac{e^{-\sqrt{2}r}}{\sqrt{r}},\quad r\to\infty. \tag{27}$$

We solved Eq. (25) numerically for $N=1$ and got $B_1\approx 0.9$ and $A_1\approx 1.6$.

To find the vortex solution at $N>1$, it is more convenient to use the new function $v_N(r)=g_N^{1/N}(r)$ that satisfies the equation

$$v_N''=\frac{v_N'^2}{v_N}-\frac{v_N'}{r}+\frac{1}{N}v_N^{2N+1}-\frac{1}{N}v_N \tag{28}$$

and has a linear behavior $\sim B_N^{1/N}r$ at $r\to 0$. The analytical expression for $g_N(r)$ at $N\gg 1$ was obtained in Ref. 4. In dimensionless units (9) it is written as

$$g_N=\left(\frac{r}{r_N}\right)^n e^{-(1/4)(r^2-r_N^2)},\quad r<r_N. \tag{29}$$

The size of the vortex core

$$r_N\approx\sqrt{2N} \tag{30}$$

is estimated from that, the almost uniform magnetic field $h_0=1$, distributed inside the vortex area πr_N^2 results to the flux $2\pi N$.

C. Separated vortices and diluted lattice

The magnetic flux of slightly overlapping vortices can be written as the superposition of fluxes of separate vortices,

$$b(\mathbf{r})=\sum_i b_N(\mathbf{r}-\mathbf{r}_i)=\sum_i\{1-g_N^2(i)\}, \tag{31}$$

where $g_N(i)=g_N(|\mathbf{r}-\mathbf{r}_i|)$ is the solution of Eq. (25). Then, the amplitude of the order parameter is written as

$$|\psi(\mathbf{r},\mathbf{r}_1,\ldots,\mathbf{r}_N)|^2=1-b(\mathbf{r})=1+\sum_i\{g_N^2(i)-1\}. \tag{32}$$

D. Vortex bunch

Consider now the group of N-vortices located close to the origin such that $|\mathbf{r}_i|\ll 1$. This vortex bunch can be viewed as the N-quanta vortex $g_N(r)$ with the split core. By direct substitution, one proves that the corresponding solution of Eq. (23) within the accuracy $O(\max|\mathbf{r}_i|^2)$ is given by

$$\varphi(\mathbf{r},\mathbf{r}_1,\ldots,\mathbf{r}_N)=\frac{1}{N}\sum_i \varphi_N(\mathbf{r}-\mathbf{r}_i)\approx\varphi_N(r)+\frac{1}{2N}\sum_i (\mathbf{r}_i\nabla)^2\varphi_N(r), \tag{33}$$

where

$$\varphi_N(r)=\ln|g_N(r)|,\quad \varphi(\mathbf{r},\mathbf{r}_1,\ldots,\mathbf{r}_N)=\ln|\psi(\mathbf{r},\mathbf{r}_1,\ldots,\mathbf{r}_N)|;$$

the origin being taken in the gravity center such that $\Sigma_i\mathbf{r}_i=0$.

With the same accuracy the order parameter is written as

$$|\psi(\mathbf{r},\mathbf{r}_1,\ldots,\mathbf{r}_N)|=g_N(r)+\frac{1}{2N}g_N(r)\sum_i (\mathbf{r}_i\nabla)^2\ln g_N(r). \tag{34}$$

E. Dense lattice

The order parameter of the dense 1-quanta vortex lattice is presented by the Abrikosov solution close to H_{c2}

$$\psi_0(\mathbf{r})=A(\overline{b})\,\theta(\overline{z}\sqrt{\overline{b}\tau''/2\pi},\tau)e^{-\overline{b}y^2/2}, \tag{35}$$

where $\tau=\tau'+i\tau''=a_2e^{i\alpha}/a_1$ is the geometrical parameter of the lattice cell (for square lattice $\tau=i$, for triangular lattice: $\tau=e^{i\pi/3}$) and θ is the Jacobi theta function

$$\theta(\overline{z},\tau)=2\sum_{n=0}^{\infty}(-1)^n\exp[i\pi\tau(n+1/2)^2]\sin[\pi(2n+1)\overline{z}]. \tag{36}$$

The function $\psi_0(\mathbf{r})$ satisfies the linear equation

$$\overline{b}\nabla^2\ln|\psi_0|=-1+2\pi\sum\delta(\mathbf{r}-\mathbf{r}_i) \tag{37}$$

that close to H_{c2} coincides with the BJR equation in the limit $\langle|\psi|^2\rangle\to0$, $\overline{b}\to1$. To find the normalization coefficient $A(\overline{b})\sim(1-\overline{b})^{1/2}$, one should treat the nonlinear part of the BJR equation as a perturbation.

The N-quanta lattice solution with a unit cell area $2\pi N$ can be written in an analogous way as

$$\psi_0(\mathbf{r})=A_N(\overline{b})\,\theta^N(\overline{z}\sqrt{\overline{b}\tau''/2\pi N},\tau)e^{-\overline{b}y^2/2}. \tag{38}$$

F. Arbitrary lattice (numerical solution)

We performed the numerical integration of the BJR equation for square and triangular vortex lattices with $N=1,2$ in the whole interval of $0<\overline{b}<1$ and presented it in a more suitable form. First we pick the zeros of the order parameter via the special multiplier $\psi_0(\mathbf{r})$ that was taken as Eq. (35) for $N=1$ or as Eq. (38) for an arbitrary N and present the order parameter in the form $\psi(\mathbf{r}=)|\psi_0(\mathbf{r})|\cdot|\psi'(\mathbf{r})|$. The new equation for function $|\psi'(\mathbf{r})|$ has no singular δ-function term and is written as

$$\frac{1}{2}\nabla^2\ln|\psi'|^2=|\psi_0|^2|\psi'|^2-(1-\overline{b}). \tag{39}$$

Taking $\varphi'=\ln|\psi'|$ we present Eq. (39) in the form

$$\nabla^2\varphi'=|\psi_0|^2e^{2\varphi'}-(1-\overline{b}). \tag{40}$$

This nonlinear Poisson-like equation can have a periodic solution only if the electroneutrality condition is satisfied,

$$1-\overline{b}=\langle|\psi_0|^2e^{2\varphi'}\rangle. \tag{41}$$

Taking into account Eq. (41) and performing the rescaling $\mathbf{r}\to\mathbf{r}\cdot(2\pi N/\overline{b})^{1/2}$ we map Eq. (40) onto

$$\nabla^2\varphi'=\Lambda\left(\frac{|\psi_0(\mathbf{r})|^2e^{2\varphi'}}{\langle|\psi_0(\mathbf{r})|^2e^{2\varphi'}\rangle}-1\right), \tag{42}$$

which is defined for the parallelogram of fixed area $S=1$ with periodic boundary conditions. The parameter of the equation

$$\Lambda=2\pi N\left(\frac{1}{\overline{b}}-1\right) \tag{43}$$

varies from 0 at H_{c2} to ∞ at H_{c1}.

The problem was solved for the square and triangular vortex lattices with $N=1,2$ using the Matlab PDE toolbox by the finite element method with the adaptive mesh refinement and with the rapidly converging Gauss-Newton iterations that were used to account for the nonlinear right-hand side of Eq. (42). For details of the numerical method, see Ref. 31. The obtained solutions were verified by substituting them back to Eq. (42).

G. Normal-superconducting interface

The profile of the NS interface is usually considered in the two limits $\kappa\to\infty$ or $\kappa\to0$. It appears, however, that the NS profile can be found *exactly* at $\kappa=1/\sqrt{2}$ by integration of Eq. (23) that in the 1D case looks like

$$\varphi''=e^{2\varphi}-1. \tag{44}$$

The first integral of Eq. (44)

$$(\varphi')^2=e^{2\varphi}-2\varphi-1 \tag{45}$$

alternatively can be written as

$$(|\psi|')^2=|\psi|^4-|\psi|^2+(1+\ln|\psi|^2). \tag{46}$$

The integration constants in Eqs. (45) and (46) was chosen to satisfy the NS interface boundary conditions

$$|\psi|=0,\ d|\psi|/dx=0\ \text{ when }\ x\to-\infty, \tag{47}$$

$$|\psi|=1,\ d|\psi|/dx=0\ \text{ when }\ x\to\infty.$$

Further integration of Eq. (46) gives the implicit form of $|\psi(x)|$ at the NS interface

TABLE I. The terms of the extended GL functional F, their dimensionless counterparts, and the coefficients in the perturbation functional f. The last two columns give the microscopic BCS values of coefficients for clean and dirty superconductors.

F	f	Coefficient	Clean limit	Dirty limit
$\frac{u}{3}\|\Psi\|^6$	$-t\upsilon\|\psi\|^6$	$\upsilon=2\alpha_1\kappa^2 u/3g^2$	$\upsilon=-\vartheta^a/2\approx-0.23$	
$R'\|\Psi\|^2\|\mathbf{D}\Psi\|^2$	$-t\rho'\|\psi\|^4(1-\|\psi\|^2)$	$\rho'=\alpha_1 R'/2gK$	$\rho'=-\vartheta\approx-0.45$	$\rho'=-\pi^2/21\zeta(3)\approx-0.39$
$R''(\nabla\|\Psi\|^2)^2$	$-t\rho''\|\psi\|^4(1-\|\psi\|^2)$	$\rho''=\alpha_1 R''/gK$	$\rho''=-\vartheta/2\approx-0.23$	$\rho''=-\pi^2/42\zeta(3)\approx-0.20$
$P\|\mathbf{D}^2\Psi\|^2$	$-t\mu\|\psi\|^2(1-\|\psi\|^2)^2$	$\mu=\alpha_1 P/2\kappa^2K^2$	$\mu=-9\vartheta/5\approx-0.82$	$\mu=-28\zeta(3)/\pi^4\approx-0.35$
$LB^2\|\Psi\|^2$	$-t\lambda(\|\psi\|^2-\|\psi\|^4)$	$\lambda=4\pi\alpha_1 L/g$	$\lambda=-9\vartheta/5\approx-0.82$	$\lambda=-36T/5\pi s_2\to0$
$Q\,\mathrm{rot}^2\,\mathbf{B}$	$-t\tau\|\psi\|^4(1-\|\psi\|^2)$	$\tau=4\pi\alpha_1 Q/2\kappa^2K$	$\tau=-3\vartheta/5\approx-0.27$	$\tau=-12T/5\pi s_2\to0$

[a] $\vartheta=31\zeta(5)/49\zeta^2(3)\approx0.454$.

$$x=\int^{|\psi|}\frac{dy}{\sqrt{y^4-y^2(1+\ln y^2)}}. \tag{48}$$

This result was first obtained by Dorsey[32] by integration of the complete set of GL equations.

V. PERTURBATION THEORY

To find the most stable configuration of vortices beyond the infinitely degenerate point $\gamma=0$ and $h_0=1$ of Bogomolnyi functional (17), we construct the secular perturbation functional that acts on the (zero order) degenerate solutions $|\psi(\mathbf{r};\mathbf{r}_1,\ldots,\mathbf{r}_n)|$ of Eq. (21) and selects the vortex configuration $\mathbf{r}_1,\ldots,\mathbf{r}_n$ having the lowest energy.

The perturbation for γ and h were given already by the two last terms in Eq. (17). To find the perturbation for t one should extend the GL functional to low temperatures. Tewordt[13,14,16] and Newman and Tewordt[15] were the first who proposed the complete form of such an extension. We will use the analogous functional given in a more recent publication:[21]

$$\begin{aligned}\mathcal{F}=&a|\Psi|^2+\frac{g}{2}|\Psi|^4+K|\mathbf{D}\Psi|^2\\&+\frac{B^2}{8\pi}-\frac{BH_0}{4\pi}+\frac{u}{3}|\Psi|^6+R'|\Psi|^2|\mathbf{D}\Psi|^2\\&+R''(\nabla|\Psi|^2)^2+P|\mathbf{D}^2\Psi|^2\\&LB^2|\Psi|^2+Q\,\mathrm{rot}^2\,\mathbf{B}.\end{aligned} \tag{49}$$

The last term $\mathrm{rot}^2\,\mathbf{B}$ was written in Ref. 21 in the equivalent form $-i\,\mathrm{rot}\,\mathbf{B}(\bar{\Psi}\mathbf{D}\Psi-\Psi\bar{\mathbf{D}}\bar{\Psi})$.

To account for all the perturbations of the order of t, one should assume that the coefficients u, R', R'', P, L, and Q are temperature independent whereas coefficients α, g, and K are expanded in t as

$$\begin{aligned}\alpha&=(\alpha_1+\alpha_2 t)t,\\g&=g_0+g_1 t,\\K&=K_0+K_1 t.\end{aligned} \tag{50}$$

The microscopic BCS values of these coefficients are given in the Appendix.

The combination $g^{1/2}/K$ that enters in Eq. (17) as defined by Eq. (6) parameter κ becomes now temperature dependent. We keep a notation $\kappa=(1+\gamma)/\sqrt{2}$ for the temperature independent part of Eq. (6) and take $\sigma t/\sqrt{2}$ with

$$\sigma=g_1/g_0-2K_1/K_0 \tag{51}$$

as a contribution to Eq. (6) that is linear in t. Therefore the third term in Eq. (17) contains both the perturbation in γ and in t and is written as

$$(\gamma+\sigma t)(|\psi|^2-1)^2. \tag{52}$$

Other perturbation terms of Eq. (49) can be substantially simplified if one takes into account that they are operating with solutions of the BJR equation. The final form of these terms in dimensionless variables and corresponding dimensionless coefficients are given in Table I. We present also the numerical values of these coefficients calculated from the microscopic BCS theory given in the Appendix. We comment now on how the perturbation terms were obtained.

(1) The term $P|\mathbf{D}^2\Psi|^2$ is rewritten in dimensionless units as

$$\begin{aligned}&-t\mu|2[(\partial-ia)(\bar{\partial}-i\bar{a})+(\bar{\partial}-i\bar{a})(\partial-ia)]\psi|^2\\&\quad=-t\mu|4(\partial-ia)(\bar{\partial}-i\bar{a})\psi+2i(\partial\bar{a}-\bar{\partial}a)\psi|^2.\end{aligned} \tag{53}$$

Because of Eqs. (18) and (19), the first term in brackets vanishes and the second term is equal to

$$-t\mu b^2|\psi|^2=-t\mu|\psi|^2(1-|\psi|^2)^2. \tag{54}$$

(2) The term $R'|\Psi|^2|\mathbf{D}\Psi|^2$ is rewritten in dimensionless units as

$$\begin{aligned}&-2t\rho'|\psi|^2[2|(\partial-ia)\psi|^2+2|(\bar{\partial}-i\bar{a})\psi|^2]\\&\quad=-2t\rho'[4t|\psi|^2|(\bar{\partial}-i\bar{a})\psi|^2-ia\bar{\partial}|\psi|^4+i\bar{a}\partial|\psi|^4].\end{aligned} \tag{55}$$

The first term in brackets vanishes and the other two can be integrated by parts. This leads to

TABLE II. Coefficients of the perturbation functional f that are collected from the dimensionless terms of Table I, their theoretical BCS values in the clean and dirty superconductors and their experimental estimation in TaN.

c_i	Clean	Dirty	TaN
$c_2=2\sigma+\mu+\lambda$	0.37	-0.35	
$c_4=-\sigma+\rho'+\rho''+\tau-2\mu-\lambda$	0.50	0.10	0.30
$c_6=\upsilon-\rho'-\rho''+\mu-\tau$	-0.09	0.01	-0.15

$$-t\rho'|\psi|^4\cdot 2i(\overline{\partial a}-\partial\overline{a})=-t\rho' b|\psi|^4=-t\rho'|\psi|^4(1-|\psi|^2). \tag{56}$$

(3) The term $Q\,\mathrm{rot}^2\,\mathbf{B}$ in dimensionless units is rewritten as

$$-t\tau\,\mathrm{rot}^2(\mathbf{z}b)=-t\tau(\nabla|\psi|^2)^2. \tag{57}$$

Multiplying Eq. (21) by $|\psi|^4$ and integrating by parts we find that $(\nabla|\psi|^2)^2$ can be substituted as

$$(\nabla|\psi|^2)^2\rightarrow|\psi|^4-|\psi|^6, \tag{58}$$

the same substitution was also done for the term $R''(\nabla|\Psi|^2)^2$.

Collecting all the above contributions together and omitting the nonessential constant contribution $1+\gamma+\sigma t-h_0$, we come to the resulting perturbation functional

$$f'=(h_0-h_{c2})|\psi|^2+(\gamma-c_4t)|\psi|^4-c_6t|\psi|^6, \tag{59}$$

where parametersc_i are given in Table II. The instability field

$$h_{c2}=1+2\gamma+c_2t. \tag{60}$$

corresponds to the *upper critical field* that we discuss below.

The perturbation functional (59) is the principal result of the present work. It allows to calculate the properties of superconductor with low γ and select the most stable vortex configuration at given γ, h_0, and t. Although functional (59) resembles the extended form of the GL functional, it is defined for the restricted set of infinitely degenerate vortex solutions $|\psi(\mathbf{r};\mathbf{r}_1,\ldots,\mathbf{r}_n)|$ of BJR equation (21). The important advantage of the functional (59) is that it depends only on few parameters, h_{c2}, c_4, and c_6 that are the combinations of the coefficients of the extended GL functional (49) as given in Table II. Moreover, it is not necessary at all to know the coefficients in the starting functional (49). These parameters can be considered as phenomenological ones. As will be shown in Sec. VII they can be found from experiment.

The occurring vortex state depends on the sign and the relative strength of the coefficients $\gamma-c_4t$ and $-c_6$ that can be positive or negative since $t<0$ and the parameter γ changes sign when κ goes though $1/\sqrt{2}$. The realistic values of c_4 and c_6 will be discussed in Sec. VII.

(i) When both $\gamma-c_4t$ and $-c_6t$ are positive, the magnetic behavior of the superconductor corresponds to the generic scenario for a superconductor of type II. The dense vortex lattice (35) appears continuously from the normal state $|\psi|=0$ at upper critical field h_{c2} when the quadratic term $(h_0-h_{c2})|\psi|^2$ in Eq. (59) becomes unstable. The amplitude $\Delta^2=\langle|\psi(\mathbf{r})|^2\rangle$ of the vortex state and the intervortex distance increase with decreasing applied field. Below the *low critical field* h_{c1} that will be calculated in Sec.VI B, all the vortices continuously leave the superconductor and the uniform Meissner state with $|\psi|=1$ becomes stable.

(ii) When both $\gamma-c_4t$ and $-c_6t$ are negative, the functional (59) corresponds to a type-I superconductor. There are only two competing local minima of Eq. (59): the normal state with $|\psi|=0$ and energy

$$f_n'=0, \tag{61}$$

and the uniform superconducting Meissner state with $|\psi|=1$ and energy

$$f_s=h_0-h_{c2}+\gamma-(c_4+c_6)t. \tag{62}$$

The discontinuous transition between them occurs at the *thermodynamic critical field* h_c

$$h_c=1+\gamma+(c_2+c_4+c_6)t. \tag{63}$$

that is found by equating Eqs. (61) and (62).

(iii) We investigate the case when the coefficients $\gamma-c_4t$ and $-c_6t$ have different signs in Sec. VII. It will appear that, depending on the situation, both *N*-*V* and *V*-*S* transition can be either continuous (as in conventional superconductors with $\kappa\gg1/\sqrt{2}$) or discontinuous. This situation is accessible experimentally either by variation of γ or by variation of t.

VI. VORTEX STATE: ENERGY AND CRITICAL FIELDS

A. Energy of the vortex lattices and higher critical field

The energy of the regular *N*-quanta lattice (59) can be written in terms of the amplitude of the order parameter $\Delta^2=\langle|\psi|^2\rangle$ as:

$$f'=(h_0-h_{c2})\Delta^2+(\gamma-c_4t)\beta_4(\Delta)\Delta^4-c_6t\beta_6(\Delta)\Delta^6, \tag{64}$$

where $\beta_n^{(N)}(\Delta)$ are the structural factors

$$\beta_n^{(N)}(\Delta)=\frac{\langle|\psi|^n\rangle}{\langle|\psi|^2\rangle^{n/2}} \tag{65}$$

that depend both on the amplitude Δ and on the lattice geometry.

Minimization of Eq. (64) over Δ gives the complete information about thermodynamic and magnetic properties of the vortex lattice in a superconductor with $\kappa\sim1/\sqrt{2}$ provided the dependencies $\beta_n^{(N)}(\Delta)$ are known. We found $\beta_n^{(N)}(\Delta)$ in the whole region of $\Delta(0<\Delta<1)$ using the numerical solutions of Eq. (21) for square and triangular vortex lattices with $N=1{,}2$ outlined in Sec. IV F. The results are shown in Fig. 1 as functions of magnetic induction

$$\overline{b}=1-\Delta^2. \tag{66}$$

The values of $\beta_n^{(1,2)}$ at $\Delta\rightarrow0$ (i.e. in vicinity of h_{c2}) are given in Table III. The parameter $\beta_4^{(N)}(0)$corresponds to the

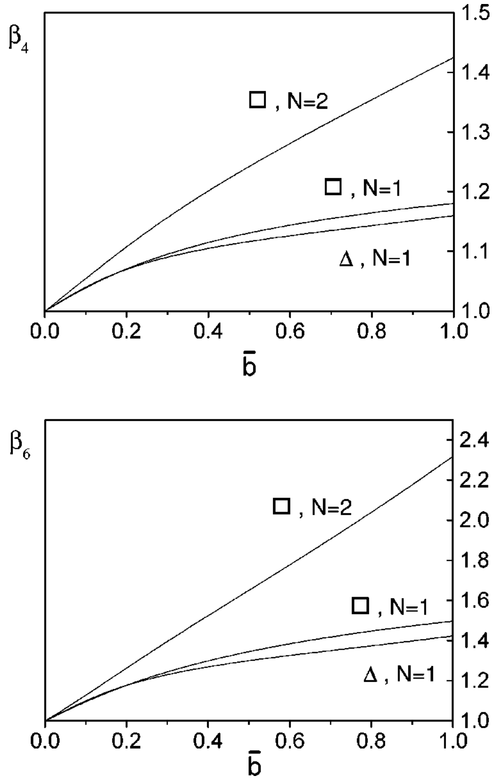

FIG. 1. Structural factors $\beta_4=\langle|\psi|^4\rangle/\langle|\psi|^2\rangle^2$ and $\beta_6=\langle|\psi|^6\rangle/\langle|\psi|^2\rangle^3$ for triangle and square N-quanta vortex lattices as functions of the average magnetic induction $\overline{b}$.

parameter β introduced in the original publication of Abrikosov.[5] Close to h_{c1} (where $\Delta\rightarrow 1$) the factors $\beta_n^{(N)}$ tend to 1. The corresponding asymptotic expression will be given in Sec. VI B.

The functional (64) close to h_{c2} can be interpreted as a Landau expansion of the vortex state energy over the amplitude Δ. When $\gamma>c_4t$ the quartic term in Δ is positive and the conventional second-order transition occurs at h_{c2}. When $\gamma<c_4t$ the transition occurs in a discontinuous way either to the finite-amplitude vortex state or directly to the Meissner state. The concrete realization of this transition depends on the relative values of c_6 and c_4 and will be discussed in Sec. VII.

The condition

TABLE III. Structural factors $\beta_n^{(N)}=\langle|\psi|^n\rangle/\langle|\psi|^2\rangle^{n/2}$ of the $N=1,2$ quanta square and triangular vortex lattices close to H_{c2} and structural factors $\zeta_n^{(N)}=\langle 1-g^n\rangle/2\pi N$ of one- and two-quanta vortices.

	$N=1$		$N=2$	
	Δ	$\Box$	Δ	$\Box$
$\beta_4^{(N)}$	1.16	1.18	1.34	1.43
$\beta_6^{(N)}$	1.42	1.50	1.95	2.32
$\zeta_4^{(N)}$	1.58		1.45	
$\zeta_6^{(N)}$	2.00		1.75	
$\zeta_8^{(N)}$	2.34		1.99	

$$\gamma-c_4t=0 \tag{67}$$

defines the tricritical point T_2 where the discontinuity of the N-V transition appears. The discontinuity field h_{c2}^* is larger than the critical field h_{c2}.

The functional (64) can be alternatively written in terms of $\overline{b}$ as

$$f'=(2\gamma+c_2t)(h_0-1)+(h_0-h_{c2})(h_{c2}-\overline{b})+(\gamma-c_4t)\beta_4(\overline{b})(h_{c2}-\overline{b})^2-c_6t\beta_6(\overline{b})(h_{c2}-\overline{b})^3. \tag{68}$$

Minimization of f' over $\overline{b}$ gives the induction $\overline{b}(h_0)$ and the lattice energy $f'(h_0)$. Comparing the energies of square and triangular lattices with $N=1,2$ at given h_0 ($h_{c1}<h_0<h_{c2}$), we established that the *one-quanta triangular vortex lattice* always possess the lowest energy. However, close to h_{c1} the energies of different lattices coincide within the calculation accuracy and this conclusion becomes less certain.

B. Diluted lattice low critical field and vortex interaction

1. Energy of the diluted vortex lattice

We consider now the diluted lattice of slightly overlapping N-quanta vortices assuming that the distance l between them is much larger than the coherence length (i.e. $l\gg 1$). Such a limit usually occurs close to the low critical field h_{c1}. In this approximation the energy of the system is written as

$$\overline{f'}=f'_s+\frac{\overline{b}}{2\pi N}\varepsilon_N+\frac{m}{2}\frac{\overline{b}}{2\pi N}U_{int}(l)-h_0\overline{b}, \tag{69}$$

where the background energy of the uniform Meissner state f'_s is given by Eq. (62), ε_N is the one-vortex energy, $\overline{b}/2\pi N$ is the density of vortices, and $-h_0\overline{b}$ is the interaction of the vortex with an external field. The term $U_{int}(l)$ represents the interaction between the nearest-neighbor vortices. The factor m gives the lattice coordination number $m=6$ for the triangular lattice and $m=4$ for the square lattice. The inter-vortex distance l is uniquely related with the vortex concentration $2\pi N/\overline{b}$ and the geometry of the lattice as

$$l_{\Box}=(2\pi N/\overline{b})^{1/2}, \quad l_{\Delta}=(4\pi N/\overline{b}\sqrt{3})^{1/2}. \tag{70}$$

The type of the V-S transition depends on the sign of the long-range vortex interaction $U_{int}(l)$ that, as will be shown below, can be repulsive or attractive.

When $U_{int}(l)>0$ the situation is the same as for a superconductor of type II: the V-S transition occurs in a continuous way at the low critical field h_{c1} that is calculated from the vortex energy ε_N. The latter can be written on the basis of Eq. (59) as

$$\varepsilon_N=2\pi N[(1+2\gamma+c_2t)-\zeta_4^{(N)}(\gamma-c_4t)+\zeta_6^{(N)}c_6t]. \tag{71}$$

The structural factors for the N-quanta vortex

$$\zeta_n^{(N)}=\frac{1}{N}\int_0^\infty (1-g_N^n)r\,dr \tag{72}$$

are found from integration of the numerical solution $g_N(r)$ of Eq. (25) and are given in Table III. Note also that

$$\zeta_2^{(N)}=\frac{\overline{b}}{2\pi N}=1. \tag{73}$$

The factors $\zeta_n^{(N)}$ for large N will be calculated in Sec. VI C. The lattice factors $\beta_n^{(N)}$ [Eq. (65)] can be expressed via $\zeta_n^{(N)}$ as

$$\beta_n^{(N)}=\frac{1-\zeta_n^{(N)}\overline{b}}{(1-\overline{b})^{n/2}}\quad(\overline{b}\to 0). \tag{74}$$

The N-quanta vortices penetrate into the sample when the positive energy ε_N required for the vortex creation is compensated by the negative magnetic contribution $-h_0\overline{b}$, i.e., above the critical field

$$h_{c1}^{(N)}=\frac{\varepsilon_N}{2\pi N}=1+(2-\zeta_4^{(N)})\gamma+(c_2+\zeta_4^{(N)}c_4+\zeta_6^{(N)}c_6)t. \tag{75}$$

The low critical field is defined as the lowest field for which the penetration of vortices becomes favorable,

$$h_{c1}=\min\{h_{c1}^{(N)}\}_N. \tag{76}$$

It appears that only the 1-quanta vortices can appear in a continuous way since the condition of formation of 2-quanta vortices written as $h_{c1}^{(2)}<h_{c1}^{(1)}$ or as

$$\gamma>(c_4+1.89c_6)t \tag{77}$$

is weaker than the condition of continuity of V-S transition: $U_{int}(l)>0$, derived below [inequality (79)].

The vortices penetrate inside a superconductor until the repulsive interaction counterbalances the energy gain. The penetrated flux is determined by minimization of Eq. (69) over $\overline{b}$ that alternatively can be written as

$$\overline{f'}=f_s'+\left[h_{c1}-h_0+\frac{m}{4\pi N}U_{int}\{l(\overline{b})\}\right]\overline{b}, \tag{78}$$

where the dependence $l(\overline{b})$ is given by Eq. (70).

When $U_{int}(l)<0$, the transition from the Meissner phase occurs either to the finite-density vortex state or directly to the normal-metal state in a discontinuous way that is manifested by the jump of magnetization. The detailed scenario of the transition depends on the energy balance between these three phases and will be discussed in Sec. VII.

The situation is simplified however near the tricritical point T_1 where the long-range part of $U_{int}(l)$ changes its sign from positive to negative. As will be shown in Sec. VI B 2 the short-range vortex interaction in this region is still repulsive. The minimum of $U_{int}(l)$ lies at $l\gg 1$ and one can apply the nearest-neighbor approximation (78). The discontinuity field h_{c1}^{*} is smaller than h_{c1}.

2. Vortex interaction

The vortex interaction is known to be repulsive in a type-II superconductor ($\gamma\gg 0$) and attractive in a type-I superconductor ($\gamma\ll 0$). In this section we calculate the interaction energy $U_{int}(l)$ of two N-quanta vortices located at $\mathbf{r}_{1,2}=\pm\boldsymbol{l}/2$ at the intermediate values of γ. The numerical part of this problem is based on the solution of the BJR equation (21) with the right-hand term $2\pi N\delta(\mathbf{r}-\mathbf{r}_1)+2\pi N\delta(\mathbf{r}-\mathbf{r}_2)$ and on substitution of this solution into the perturbation functional (59). We give the analytical treatment of this problem in cases of slightly overlapped ($l\gg 1$) and of strongly overlapped ($l\ll 1$) vortices. As a result we obtain that vortices begin to attract each other at large distances when

$$\gamma<(c_4+3c_6)t. \tag{79}$$

Below this instability the vortex interaction has a long-range attractive and short-range repulsive character and vortices form a bounded state. The inequality (79) presents also the condition of discontinuity of V-S transition.

With the decrease of γ, the equilibrium distance l_0 varies from infinity to zero. Below another instability point at

$$\gamma<\left(c_4+1.5\frac{\zeta_8^{(N)}-\zeta_6^{(N)}}{\zeta_6^{(N)}-\zeta_4^{(N)}}c_6\right)t \tag{80}$$

the interaction is purely attractive and vortices are stuck together, with the formation of $2N$-quanta vortex. The results about the short-range vortex interaction can not be directly applied to study the vortex lattice since the nearest-neighbor approximation (78) is not applicable at low vortex separation l.

The calculations of the long-range vortex interaction given below are compatible with calculations of the vortex interaction given in Ref. 17 in a more bulky way. Consider for simplicity the case of two 1-quanta vortices. When the distance between the vortices is large ($l\gg 1$), it is more suitable to describe the vortices in terms of slightly overlapping magnetic fluxes produced by these vortices

$$b_\pm=1-g_1^2(|\mathbf{r}\pm\boldsymbol{l}/2|), \tag{81}$$

as was discussed in Sec. IV C.

The vortex energy is provided by the terms $|\psi|^2$, $|\psi|^4$, and $|\psi|^6$ in the functional (59) that can be evaluated as

$$|\psi|^2=1-b_+-b_-, \tag{82}$$

$$|\psi|^4=(1-b_+-b_-)^2=(1-b_+)^2+(1-b_+)^2-1+2b_+b_-, \tag{83}$$

and

$$|\psi|^6=(1-b_+-b_-)^3=(1-b_+)^3+(1-b_+)^3 -1+6b_+b_--3b_-^2b_+-3b_+^2b_-. \tag{84}$$

Only $|\psi|^4$ and $|\psi|^6$ terms contain the interaction parts b_+b_-, $b_+^2b_-$, and $b_+b_-^2$. With the help of Eq. (26), the overlapping contribution $\langle b_+b_-\rangle$ can be estimated with exponential accuracy as $u(l)e^{-4l}$ where $u(l)$ is a slow function of l. This term is more important at $l \gg 1$ than terms $\langle b_+ b_-^2 \rangle$ and $\langle b_+^2 b_- \rangle$ decaying like e^{-6l}.

Substitution of $\langle b_+ b_- \rangle$ from Eqs. (83) and (84) into Eq. (59) gives the long-range interaction energy per vortex:

$$U_{int}(l) = [\gamma - (c_4 + 3c_6)t] \cdot u(l) e^{-4l}. \quad (85)$$

This interaction is attractive when condition (79) is satisfied.

Consider now the short-range part of the vortex interaction. When vortices are located close to each other ($l \ll 1$), their order parameter is given by Eq. (34),

$$|\psi(\mathbf{r})| = g_2(r) + \frac{1}{8} g_2(r)(\mathbf{l}\nabla)^2 \ln g_2(r). \quad (86)$$

To calculate the vortex energy one should estimate

$$\int |\psi(\mathbf{r})|^n d^2\mathbf{r} \approx 2\pi \int g_2^n(r) r\,dr + \frac{n}{8} \int g_2^n(r) \times (\boldsymbol{l}\nabla)^2 \ln g_2(r) d^2\mathbf{r}. \quad (87)$$

Since $g_2(r)$ is an axisymmetric function, the operator $(\mathbf{l}\nabla)^2$ can be substituted by $(l^2/2)\nabla^2$. Finally, taking into account the BJR equation $\nabla^2 \ln g_2 = g_2^2 - 1$ one gets

$$\int |\psi(\mathbf{r})|^n d^2\mathbf{r} \approx 2\pi \int g_2^n(r) r\,dr + \frac{\pi n l^2}{4} (\zeta_{n+2}^{(2)} - \zeta_n^{(2)}). \quad (88)$$

The interaction energy is calculated on the basis of Eq. (59) with respect to the state where the vortex cores coincide. With the help of Eq. (88) one gets the short-range interaction energy

$$U_{int}(l) = [(\gamma - c_4 t)(\zeta_6^{(2)} - \zeta_4^{(2)}) - 1.5 c_6 t (\zeta_8^{(2)} - \zeta_6^{(2)})] \pi l^2, \quad (89)$$

This interaction is attractive when condition (80) is satisfied.

C. Energy of the normal-superconducting interface

The profile of the N-S interface is given by Eq. (48). Based on our perturbation approach, we calculate the N-S interface energy at $h_0 = h_c$ as

$$\sigma_{ns} = -(\gamma - c_4 t)\alpha_4 + c_6 t \alpha_6, \quad (90)$$

where the structural factors α_n are defined as

$$\alpha_n = \int_{-\infty}^{\infty} (|\psi|^2 - |\psi|^n) dx. \quad (91)$$

With the help of Eq. (45) these factors can be presented in the form of definite integrals

$$\alpha_n = \int_{-\infty}^{\infty} (e^{2\varphi} - e^{n\varphi}) dx = -\int_{\varphi=-\infty}^{\varphi=0} \frac{e^{2\varphi} - e^{n\varphi}}{1 - e^{2\varphi}} d\varphi_x' = \int_0^{\infty} \frac{e^{-2\eta} - e^{-n\eta}}{\sqrt{e^{-2\eta} + 2\eta - 1}} d\eta \quad (92)$$

and calculated numerically,

$$\alpha_4 \simeq 0.55, \quad \alpha_6 \simeq 0.85, \quad \alpha_8 \simeq 1.06. \quad (93)$$

Jacobs[17] has also calculated the expansion of σ_{ns} over γ and t but in a numerical way. Similar to Eq. (92), analytical expression for α_4 was done in Ref. 32.

One can now express the vortex structural factors $\zeta_n^{(N)}$ [Eq. (72)] for $N \gg 1$ via the N-S interface factors α_n. The N-quanta vortex (29) can be viewed as the cylindrical normal-state domain of radius $r_N \approx \sqrt{2N}$ surrounded by the N-S interface. The domain energy is written as

$$\varepsilon_N = \pi r_N^2 h_c + 2\pi r_N \sigma_{ns}, \quad (94)$$

where $\pi r_N^2 h_c$ is the energy of the condensate break inside the domain and $2\pi r_N \sigma_{ns}$ is the domain-wall energy. Comparison of Eqs. (94) and (71) gives

$$\zeta_n^{(N)} = 1 + \frac{\alpha_n}{\sqrt{N}}, \quad N \gg 1. \quad (95)$$

It is interesting to note that formula (95) can be extrapolated to small N with an accuracy 5–8 %.

VII. *H*-*T* PHASE DIAGRAM

We are now in a stage to discuss the properties of H-T diagram of a superconductor with $\kappa \sim 1/\sqrt{2}$. (We use again the dimensional variables.) Partially, this question was considered in Ref. 17 on the basis of Neumann-Tewordt extension of GL equations to the low temperature. The advantage of our approach is that it allows to get the structure of H-T diagram in a unified way from a simple perturbation functional (59). This functional depends on three driving parameters h_0, t, and γ that are controlled by experimental conditions and on three phenomenological parameters h_{c2}, c_4, and c_6 that can be found from an experiment based on the relations

$$\frac{H_{c2}}{H_c} = 1 + \gamma - (c_4 + c_6)t, \quad (96)$$

$$\left(\frac{dM}{dH}\right)_{H=H_{c2}} = \frac{1}{8\pi\beta_4(\gamma - c_4 t)}, \quad (97)$$

$$\frac{H_c}{H_{c1}} = 1 + (\zeta_4 - 1)\gamma + [(\zeta_4 - 1)c_4 + (\zeta_6 - 1)c_6]t, \quad (98)$$

extracted from Eqs. (60), (63), (68), and (75). The first value was also called as $\kappa_1(T)$, the second one as $4\pi\beta_4[2\kappa_2^2(T) - 1]$, and the third one as $2\kappa_3/\ln\kappa_3$.[8]

We extracted the parameters c_4 and c_6 from magnetic measurements in TaN (Ref. 26) and got $c_4 \simeq 0.30$ and $c_6 \simeq -0.15$. These parameters can be also estimated theoretically from the microscopic BCS expression for coefficients of the extended GL functional.[21] Calculations presented in the Appendix and in Tables I and II give $c_4 = 0.5$ and $c_6 = -0.09$ for clean superconductor and $c_4 = 0.1$ and $c_6 = 0.01$ for the dirty superconductor. Although these estimations do not take

TABLE IV. Characteristic points in H-T diagram of superconductor with $\gamma=\kappa^2-\frac{1}{2}$ close to zero.

Fourth-order coefficient in energy expansion <0 at	$\gamma<c_4 t$	Tricritical point T_2 where at $c_6>0$ the $H_{c2}(T)$ transition becomes discontinuous.
$H_c(T)=H_{c2}(T)$ at	$\gamma=(c_4+c_6)t$	Triple point L_2 where at $c_6>0$ the $H_c(T)$, $H^*_{c1}(T)$, and $H_{c2}(T)$ transition lines meet.
$H_{c1}(T)=H_{c2}(T)$ at	$\gamma=(c_4+1.22c_6)t$	Auxiliary point.
Short-range vortex interaction is repulsive at	$\gamma>(c_4+1.26c_6)t$	Point where 2-quanta vortex decay onto two close lying 1-quanta vortices.
$\sigma_{ns}<0$ at	$\gamma<(c_4+1.55c_6)t$	NS interface energy becomes negative.
$H_c(T)=H_{c1}(T)$ at	$\gamma=(c_4+1.75c_6)t$	Triple point L_1 where at $c_6>0$ the $H_c(T)$, $H_{c1}(T)$, and $H^*_{c2}(T)$ transition lines meet.
$H^{(1)}_{c1}(T)<H^{(2)}_{c1}(T)$ at	$\gamma>(c_4+1.89c_6)t$	Two separate one-quanta vortices are more stable than one two-quanta vortex.
Long range vortex interaction is attractive at	$\gamma<(c_4+3c_6)t$	Tricritical point T_1 where at $c_6<0$ the $H_{c1}(T)$ transition becomes discontinuous.

into account the anisotropy of TaN and the electron-phonon retardation effects in the BCS theory, they give a correct idea about the magnitude of the coefficients c_4 and c_6. We assume further that c_4 varies from 0.1 to 0.5 and c_6 from -0.2 to 0.01; the negative value of c_6 being more probable.

The H-T diagram of low-γ superconductor at given c_4 and c_6 can be obtained from comparison of relative location of critical fields (60), (63), and (75) and characteristic critical points that were calculated in Sec. VI and that are resumed in Table IV. To avoid the narrowness of the mixed-state region and to clearly demonstrate the details of the H-T diagram, we trace it in the specially normalized coordinates T/T_c and H/H_c where H_c depends on T linearly,

$$H_c=H_c'(T_c-T), \tag{99}$$

with $H_c'=(4\pi/g)^{1/2}\alpha_1/T_c$ [Eq. (7)]. The topology of the H-T diagram depends on the relative strength of the coefficients c_6 and c_4 and is provided by the only driving parameter c_6/c_4. This makes our analysis more restrictive then analysis of Ref. 17 where the six driving parameters $\kappa_{c1},\ldots,\kappa_{c6}$ were defined to consider the phase diagram.

Three possible scenario of N-S transition can be distinguished.

(i) Figure 2 corresponds to $c_6,c_4>0$ and to $\gamma<0$. Between T_c and the triple point L_1 defined by the condition $H_c(T)=H_{c1}(T)$ or

$$\gamma=(c_4+1.75c_6)t, \tag{100}$$

the superconductor behaves like superconductor of type I i.e., the discontinuous N-S transition occurs at the critical field H_c. On the left of L_1 the N-S transition occurs via an intermediate vortex state. The V-S transition occurs in a continuous way at $H=H_{c1}$ like in type-II superconductor. The N-V transition has a discontinuous character close to L_1. The discontinuity line H^*_{c2} terminates in the tricritical point T_2 defined by Eq. (67) where the fourth-order term in functional (64) becomes positive. On the left of T_2 the N-V transition occurs in a continuous way at $H=H_{c2}$ and the superconductor behaves like conventional type-II superconductor. When γ decreases, the points L_1 and T_2 are shifted to low temperatures and the superconductor becomes superconductor of type I in the whole temperature region. When γ increases, the points L_1 and T_2 are shifted to T_c. At positive γ, the superconductor has a type-II behavior.

(ii) Fig. 3 corresponds to $c_4>0$, $0>c_6>-c_4/3$ and to $\gamma<0$. Similar to case (i), the vortex state appears on the left of the triple point L_2 that is defined by the condition $H_{c2}(T)=H_c(T)$ or

$$\gamma=(c_4+c_6)t. \tag{101}$$

The N-V transition has a continuous character and occurs at $H=H_{c2}$. The type of the V-S transition is provided by the location of the tricritical point T_1 where the long-range vortex interaction changes sign [condition (79)]. The V-S transition is discontinuous between L_2 and T_1 at $H=H^*_{c1}$ and continuous on the left of T_1 at $H=H_{c1}$ .When γ decreases, the superconductor transforms to superconductor of type I whereas when γ increases above zero it becomes a superconductor of type II.

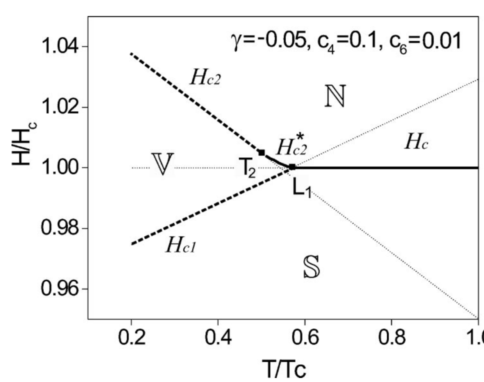

FIG. 2. H-T phase diagram of a superconductor with $c_4,c_6>0$ and with γ slightly less than zero. It includes normal (N), vortex (V), and Meissner superconducting (S) phases. Solid and dashed lines correspond to the discontinuous and continuous transitions, and dotted lines present the auxiliary critical fields. Magnetic field is measured in units of the temperature-dependent critical field $H_c=H_c'(T_c-T)$.

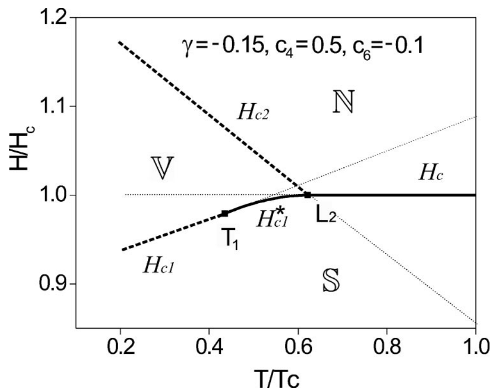

FIG. 3. The same as Fig. 2 but for $c_4>0$, $0>c_6>-c_4/3$ when γ is slightly less than zero.

(iii) Figure 4 corresponds to $c_4>0$, $-c_4/3>c_6$. This case corresponds to the experimental situation in TaN.[26] When γ is slightly less than zero [Fig. 4(a)], the H-T diagram is obtained from the diagram of case (ii) by shift of the tricritical point T_1 to the region of negative temperatures. Like in previous cases, the superconductor transforms to a superconductor of type I with decreasing γ. When γ increases, point L_2 goes to T_c and disappears at $\gamma=0$. When γ becomes positive [Fig. 4(b)] the V-S transition is continuous between T_c and the tricritical point T_1 that appears at T_c at $\gamma=0$ and is moving to the region of low temperatures with increasing γ. On the left of T_1 the V-S transition has a discontinuous

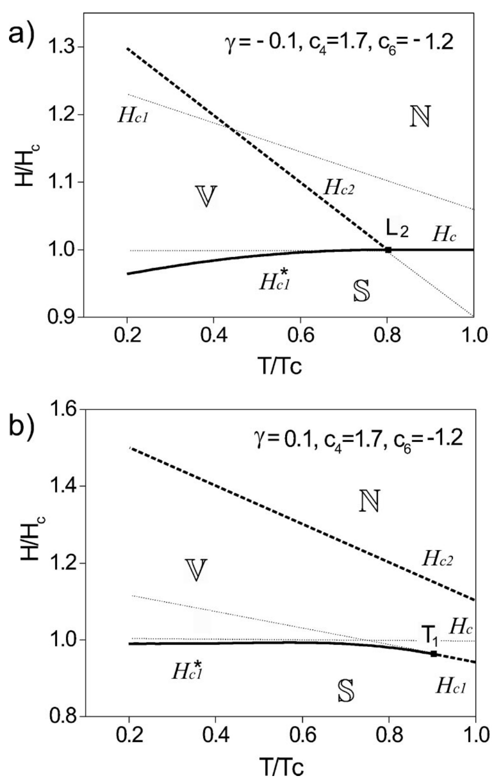

FIG. 4. The same as Figs. 2 and 3 but for $c_4>0$, $-c_4/3>c_6$ when γ is slightly less than zero (a) and when γ is slightly larger than zero (b).

character. At large γ, the phase diagram transforms to conventional H-T diagram of superconductor of type II.

ACKNOWLEDGMENTS

I am grateful to Y. N. Ovchinnikov, V. Geshkenbein, and J. Blatter for helpful discussions of the theoretical aspects and to L. Y. Vinnikov for explication of the experimental situation. I thank especially H. Capellmann for his hospitality during my stay in RWTH-Aachen. The work was done in part at the Federal University of Minas Gerais, Brazil and at the Eidgenössische Technische Hochschule, Zürich.

APPENDIX: MICROSCOPIC PARAMETERS

The microscopic BCS parameters of the extended GL functional (49) were calculated in Ref. 21. The first three coefficients do not depend on the purity of the superconductor,

$$\alpha=\nu\ln\frac{T}{T_c}, \tag{A1}$$

$$\frac{g}{2}=\nu\frac{7\zeta(3)}{16}\frac{1}{(\pi T)^2},\quad \frac{u}{3}=-\frac{\nu}{2}\frac{31\zeta(5)}{64}\frac{1}{(\pi T)^4}.$$

Here $\nu=mp_F/2\pi^2\hbar^3$ is the density of states.

Other coefficients depend on the quality of the material and can be calculated in two limit cases.

a. Clean limit

$$K=\nu\frac{7\zeta(3)}{48}\frac{v^2\hbar^2}{(\pi T)^2},\quad P=-\frac{\nu}{20}\frac{31\zeta(5)}{64}\frac{\hbar^4v^4}{(\pi T)^4}, \tag{A2}$$

$$R'=-\frac{\nu}{3}\frac{31\zeta(5)}{64}\frac{v^2\hbar^2}{(\pi T)^4},\quad R''=-\frac{\nu}{12}\frac{31\zeta(5)}{64}\frac{v^2\hbar^2}{(\pi T)^4},$$

$$Q=-\frac{1}{35\pi}\frac{31\zeta(5)}{64\zeta(3)}\frac{\hbar^2v^2}{(\pi T)^2},\quad L=-\frac{\nu}{5}\frac{31\zeta(5)}{64}\frac{e^2}{c^2\hbar^2}\frac{\hbar^4v^4}{(\pi T)^4}.$$

b. Dirty limit

$$K=\nu\frac{\pi^2}{48}\frac{v^2\hbar^2}{s_1\pi T},\quad P=-\nu\frac{7\zeta(3)}{12\times 48}\frac{\hbar^4v^4}{s_1^2(\pi T)^2}, \tag{A3}$$

$$R'=-\nu\frac{\pi^4}{12\times 48}\frac{v^2\hbar^2}{s_1(\pi T)^3},\quad R''=-\nu\frac{\pi^4}{48^2}\frac{v^2\hbar^2}{s_1(\pi T)^3},$$

$$Q=-\frac{1}{80\pi}\frac{\hbar^2v^2}{s_1s_2},\quad L=-\nu\frac{\pi^2}{80}\frac{e^2}{c^2\hbar^2}\frac{\hbar^4v^4}{s_1^2s_2\pi T},$$

where parameters s_1 and s_2 are functions of the scattering times τ, τ_1, and τ_2 in the s, p, and d channels,

$$s_1=\frac{\hbar}{2\tau_{tr}}=\frac{\hbar}{2}\left(\frac{1}{\tau}-\frac{1}{\tau_1}\right),\quad s_2=\frac{\hbar}{2}\left(\frac{1}{\tau}-\frac{1}{\tau_2}\right). \tag{A4}$$

From Eqs. (A1), (A2), and (A3) we calculate the microscopic expressions for the parameter σ defined by Eq. (51),

$$\sigma_{cl}=1,\quad \sigma_d=0, \tag{A5}$$

and for the GL parameter κ

$$\kappa_{cl}=\frac{3}{\{7\pi\zeta(3)\nu\}^{1/2}}\frac{\pi Tc}{|e|\hbar v^2},\quad \kappa_d=\frac{3\{7\zeta(3)\}^{1/2}}{\pi^2(\pi\nu)^{1/2}}\frac{cs_1}{|e|\hbar v^2} \tag{A6}$$

in clean and in dirty superconductors.

[1] E. B. Bogomolnyi, Yad. Fiz. **24**, 861 (1976) [Sov. J. Nucl. Phys. **24**, 449 (1976)]; E. B. Bogomolnyi and A. I. Vainstein, *ibid.* **23**, 1111 (1976) [**23**, 588 (1976)].
[2] L. Jacobs and C. Rebbi, Phys. Rev. B **19**, 4486 (1979).
[3] E. Akkermans and K. Mallick, Physica C **332**, 250 (2000); E. Akkermans, D. M. Gangardt, and K. Mallick, Phys. Rev. B **62**, 12 427 (2000).
[4] A. V. Efanov, Phys. Rev. B **56**, 7839 (1997).
[5] A. A. Abrikosov, Zh. Éksp. Teor. Fiz. **32**, 1442 (1957) [Sov. Phys. JETP **5**, 1174 (1957)].
[6] R. P. Hübener, *Magnetic Flux Structures in Superconductors* (Springer, New York, 1979).
[7] E. H. Brandt and U. Essmann, Phys. Status Solidi B **144**, 13 (1987).
[8] D. Saint-James, G. Sarma, and E. J. Thomas, *Type II Superconductivity* (Pergamon Press, Oxford, 1969).
[9] K. Maki, Physics (Long Island City, N.Y.) **1**, 21 (1964); **1**, 127 (1964).
[10] C. Caroli, M. Cyrot, and P. G. De Gennes, Solid State Commun. **4**, 17 (1966).
[11] K. Maki and T. Tsuzuki, Phys. Rev. **139**, A868 (1965).
[12] G. Eilenberger, Phys. Rev. **153**, 584 (1967).
[13] L. Tewordt, Z. Phys. **180**, 385 (1964).
[14] L. Tewordt, Phys. Rev. **135**, A1745 (1965).
[15] L. Neumann and L. Tewordt, Z. Phys. **189**, 55 (1966).
[16] L. Tewordt, Z. Phys. **184**, 319 (1965).
[17] A. E. Jacobs, Phys. Rev. B **4**, 3016 (1971); **4**, 3022 (1971); **4**, 3029 (1971).
[18] A. Hubert, Phys. Status Solidi B **53**, 147 (1972).
[19] S. Grossmann and Ch. Wissel, Z. Phys. **252**, 74 (1972).
[20] E. H. Brandt, Phys. Status Solidi B **77**, 105 (1976).
[21] Y. N. Ovchinnikov, Zh. Éksp. Teor. Fiz. **115**, 726 (1999) [Sov. Phys. JETP **88**, 398 (1999)].
[22] T. McConville and B. Serin, Phys. Rev. **140**, A1169 (1965).
[23] T. McConville and B. Serin, Rev. Mod. Phys. **36**, 112 (1964).
[24] J. Schelten, H. Ullmaier, and W. Schmatz, Phys. Status Solidi B **48**, 619 (1971).
[25] H. W. Weber, J. Schelten, and G. Lippmann, Phys. Status Solidi B **57**, 515 (1973).
[26] J. Auer and H. Ullmaier, Phys. Rev. B **7**, 136 (1973).
[27] T. Kinsel, E. A. Lynton, and S. Serin, Rev. Mod. Phys. **36**, 105 (1964).
[28] U. Krägeloh, Phys. Status Solidi **42**, 559 (1970).
[29] H. Träuble and U. Essmann, Phys. Status Solidi **20**, 95 (1967).
[30] N. V. Sarma, Philos. Mag. **18**, 171 (1968).
[31] *Partial Differential Equation Toolbox Users Guide* (The MathWorks, 1996), available at http://www.mathworks.com/access/helpdesk/help/toolbox/pde/pde.shtml
[32] A. T. Dorsey, Ann. Phys. (N.Y.) **233**, 248 (1993).